

Electronic Supplementary Information (ESI) for:

Developing iron-based anionic redox couples for
thermogalvanic cells: towards the replacement of the
ferricyanide/ferrocyanide redox couple

Mark A. Buckingham,^a Kristine Laws^a Edward Cross,^a Andrew J. Surman,^a and
Leigh Aldous^{a,*}

^a Department of Chemistry, Britannia House, King's College London, London,
SE1 1DB, UK

* Corresponding author: leigh.aldous@kcl.ac.uk

Contents

Figure S1 – Structures of investigated ligands

Table S1 – Table of data for initial ligand screening

Table S2 – Table of data for semi-optimisation of polycarboxylate ligands

Table S3 – Table of data for semi-optimisation of poly-aminocarboxylate ligands

Figure S2 – Au *vs* Pt CV comparison for investigated Fe(ligand) complexes

Figure S3 – Bar charts of electrochemical analysis of the Fe(ligand) complexes

Figure S4 – Bar charts of the electrochemical impedance analysis of Fe(ligand) complexes

Figure S5 – Nyquist plots (+ fitting) for all Fe(ligand) complexes

Figure S6 – UV-Vis spectra of the Fe(III), Fe(II) and Fe(III)/(II) Fe(ligand) complexes

Figure S7 – Weaver plot of the semi-optimised Fe(ligand) complexes prior to pH-optimisation

Figure S8 – Avogadro energy minimised structures for the Fe(ligand) complexes

Figure S9 – Structures of the energy minimised Fe(ligand) complexes

Table S4 – Table of costing data

Table S5 – Table of data for the cost analysis

Initial screening of carboxylate and aminocarboxylate ligands.

In an effort to generate highly charged but sustainable and safe redox couples, a range of poly-carboxylate (Figure S1(a – g)) and poly-aminocarboxylate (Figure S1(h – m)) ligands were screened.

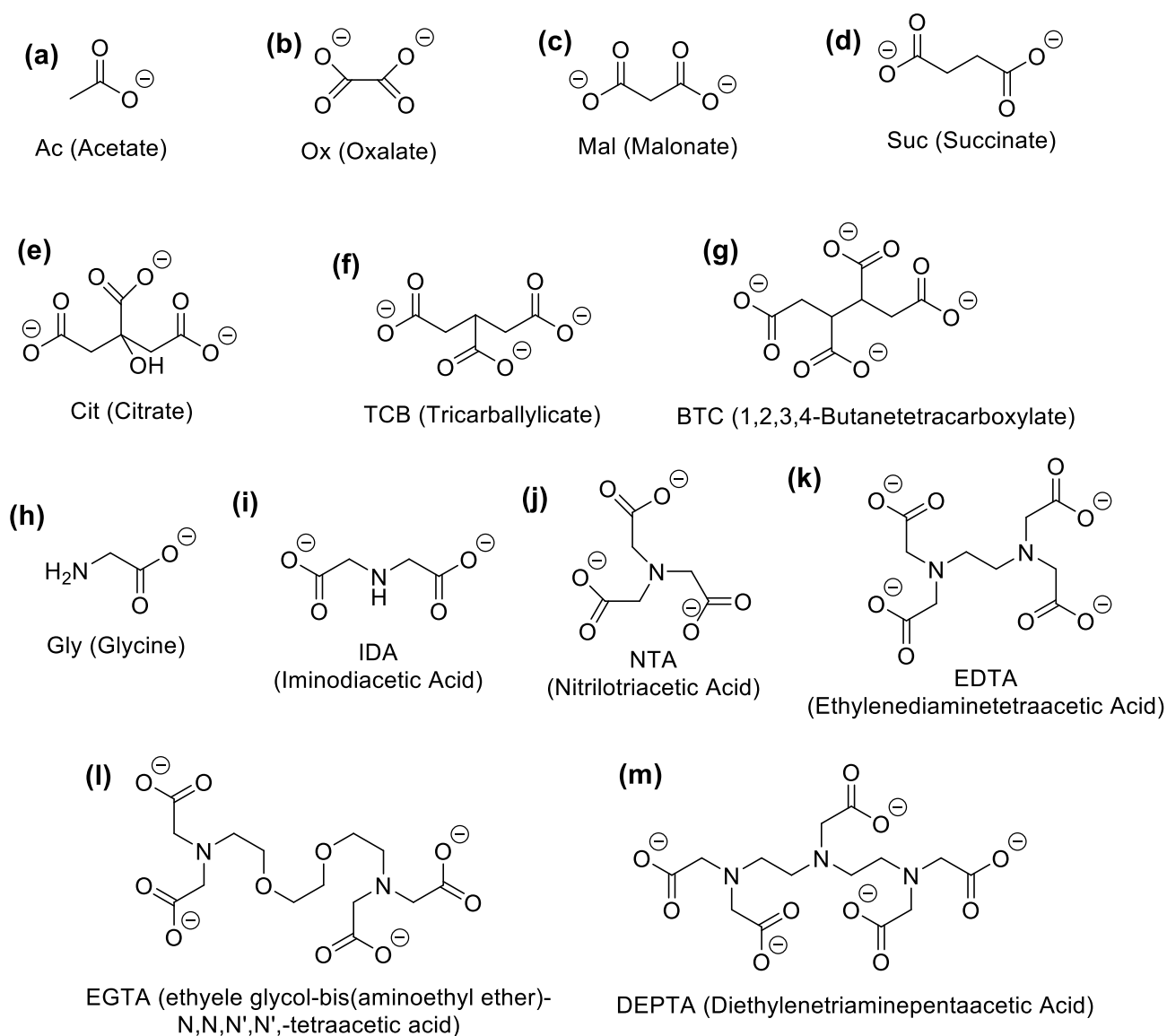


Figure S1 – Chemical structures, abbreviated name (full common name) for the anionic ligands investigated in this study.

The poly-carboxylate (Figure S1(a-g)) redox couples were screened by evaluating 50 mM FeCl₂ and 50 mM FeCl₃ in the presence of 10 equivalents (500 mM) of the carboxylate ligand, with 5 equivalents as the free acid and 5 equivalents as the conjugate sodium carboxylate. Of the 7 ligands, only 3 passed this initial screening; the thermogalvanic results for these systems are summarised in Table 1. Acetate, malonate and citrate visually complexed with the iron (based upon colour change) and importantly, significant changes in the thermoelectrochemistry were observed. The acetate and citrate both demonstrating an inversion in the entropy difference, *e.g.* the positive S_e of 0.1 M FeCl_{2/3} (+1.1 mV K⁻¹) inverted to negative S_e of -0.40 mV mV K⁻¹ upon addition of the citrate. This compares favourably with the previously reported [Fe(SO₄)₂]⁻²⁻ system ($S_e = ca. -0.29$ mV K⁻¹ for 0.3 M Fe(SO₄), 0.3 M Fe(SO₄)_{1.5} and 1.5 M Na₂SO₄).¹ The oxalate and succinate ligands were found to be sparingly soluble. Finally, the TBC and BTC ligands were soluble, but upon addition of these to the iron salt solution precipitation occurred immediately; these 4 systems were therefore eliminated from further exploration.

Table S1 – Table of data showing the corresponding thermogalvanic properties (Seebeck coefficient, S_e , short circuit current density, j_{sc} , and maximum power density, P_{max}) measured for the as-prepared Fe(ligand) solutions. These were prepared from 50 mM FeCl₂ and 50 mM FeCl₃; all polycarboxylate ligands (Ac to BTC) were measured with 5 equivalents of the carboxylic acid form and 5 equivalents of the carboxylate salt, while the polyaminocarboxylate (Gly to DEPTA) were measured using 2 equivalents of the carboxylate salt. Thermogalvanic properties were quantified in the thermogalvanic cell at an applied $\Delta T = 18$ K; n/a indicates solubility issues precluded thermogalvanic measurement.

Ligand	S_e / mV K ⁻¹	j / A m ⁻²	P_{max} / mW m ⁻²
Ac	-0.07	-0.06	0.02
Ox	n/a	n/a	n/a
Suc	n/a	n/a	n/a
Mal	+0.03	+0.07	0.01
TCB	n/a	n/a	n/a
Cit	-0.40	-0.28	0.55
BTC	n/a	n/a	n/a
Gly	n/a	n/a	n/a
IDA	-0.38	-0.98	1.84
NTA	-0.09	-0.20	0.09
EDTA	-0.20	-0.29	0.29
EGTA	-0.32	-0.42	0.67
DEPTA	-0.44	-1.48	3.25

Moving onto the poly-aminocarboxylate ligands, the free acids were consistently found to be poorly soluble; the numerous binding sites also meant less of the carboxylate conjugate base (as the sodium salt) was required. Therefore 50 mM FeCl₂ and 50 mM FeCl₃ was initially screened in the presence of 2 equivalents (200 mM) of the fully deprotonated carboxylate salts. Here, all 6 visually appeared to complex, and reassuringly 5 demonstrated negative S_e values; only glycine was unsuccessful as the resulting complex was insoluble.

Semi-optimisation of the poly-carboxylate systems

Acetate, malonate, and citrate were subjected to semi-optimisation; since the goal was a more negative S_e value, more of the conjugate base was added. As shown in Table S2, this was unsuccessful for acetate, with the resulting complex being insoluble. Malonate was dramatically improved by doubling the quantity of the carboxylate salt, with the S_e inverting from $+0.03 \text{ mV K}^{-1}$ to -0.47 mV K^{-1} , and the power increasing 260-fold. Conversely, citrate demonstrated a decrease in performance after doubling the quantity of the carboxylate salt. The semi-optimised malonate system displayed by far the highest thermogalvanic power production for the poly-carboxylate-based systems, as shown conclusively by the power curves in Figure 2(a) in the main text.

Table S2 – Table of data summarising the thermogalvanic properties for semi-optimised polycarboxylate ligand systems, achieved *via* varying the number of equivalents per Fe(II/III) and the acid:carboxylate ratio. All other conditions are as per Table S1.

Ligand	Charge	Eq. Acid	Eq. Base	S_e / mV K^{-1}	j / A m^{-2}	P_{max} / mW m^{-2}
Ac	1-	5	5	-0.07	-0.06	0.02
Ac	1-	5	10	-	-	-
Ac	1-	10	10	-	-	-
Mal	2-	5	5	+0.03	+0.07	0.01
Mal	2-	5	10	-0.47	-1.1	2.6
Cit	3-	5	5	-0.40	-0.28	0.55
Cit	3-	5	10	-0.32	-0.17	0.27

Semi-optimisation of the poly-aminocarboxylate systems

The 5 successful poly-aminocarboxylate systems were subjected to considerably more optimisation, both by increasing the quantity of the carboxylate salt, and by adding some of the free acid; the results are summarised in Table S3.

Table S3 - Table of data summarising the thermogalvanic properties for semi-optimised polyaminocarboxylate ligand systems, achieved *via* varying the number of equivalents per Fe(II/III) and the acid:carboxylate ratio. All other conditions are as per Table 1.

Ligand	Eq. Acid	Eq. Base	S_e / mV K ⁻¹	j / A m ⁻²	P_{max} / mW m ⁻²	Semi- optimised?
Glycine	0	2	Insoluble			
	2	2				
	5	5				
	5	2	+0.52	+0.18	0.50	
IDA	0	2	-0.31	-0.53	0.83	
	0	4	-0.18	-0.09	0.10	
	0	6	-0.30	-0.13	0.21	
	2	2	-0.43	-0.81	1.73	
	2*	4*	-0.38	-0.98	1.84	*
	2	6	+0.35	+0.86	1.50	
NTA	0	6	-0.45	-1.21	2.7	
	0*	5*	-0.51	-1.24	3.2	*
	0	4	-0.43	-1.13	2.4	
	0	3	-0.26	-0.45	0.59	
	0	2	-0.09	-0.20	0.09	
EDTA	0*	2*	-0.20	-0.30	0.27	
	0	3	0	0	0	
EGTA	0*	2*	-0.31	-0.45	0.70	*
	0	3	-0.48	-0.20	0.50	

DEPTA	0	3	-0.45	-1.5	3.34	
	0*	2*	-0.44	-1.5	3.24	*

Briefly, glycine could be made soluble through the introduction of more of the corresponding free acid, but only yielded a positive S_e system (+0.52 mV K⁻¹); at this stage glycine was removed from further study. IDA was the only poly-aminocarboxylate system that benefited from the addition of the corresponding acid; the S_e values varied between +0.35 and -0.43 mV K⁻¹, with the highest power achieved when there was twice as much carboxylate salt present as free acid. NTA reached peak performance with 5 equivalents of the carboxylate, whereas the larger EDTA ligand was optimised with 2 equivalents; EGTA had a higher S_e with 3 equivalents, but higher power (likely due to faster kinetics) was achieved with only 2. The largest ligand, DEPTA, displayed excellent performance with either 2 or 3 equivalents; it yielded consistently high negative S_e values, and the highest power.

The spectrum of power values demonstrated by the semi-optimised systems is demonstrated clearly by the overlay of the different power curves shown in Figure 2(b) in the main text; Fe(NTA) has the higher S_e value (*i.e.* better thermodynamics) but Fe(DEPTA) had higher power (*i.e.* faster kinetics).

The resulting values from the semi-optimised systems are summarised in Figure 3 in the main text; clearly a spectrum of negative S_e values were produced by the different ligands (Figure 3(a) in the main text). Typically, higher S_e values lead to a higher overpotential driving the cell reaction, leading to higher thermogalvanic current and power,² but as shown by Figures 3(b) and (c) in the main text (current and power, respectively) the correlation is weak here. Given this observation, the semi-optimised systems were compared using electrochemical and spectroscopic characterisation (discussed in the main text).

Au v Pt CV for Fe(ligand) complexes

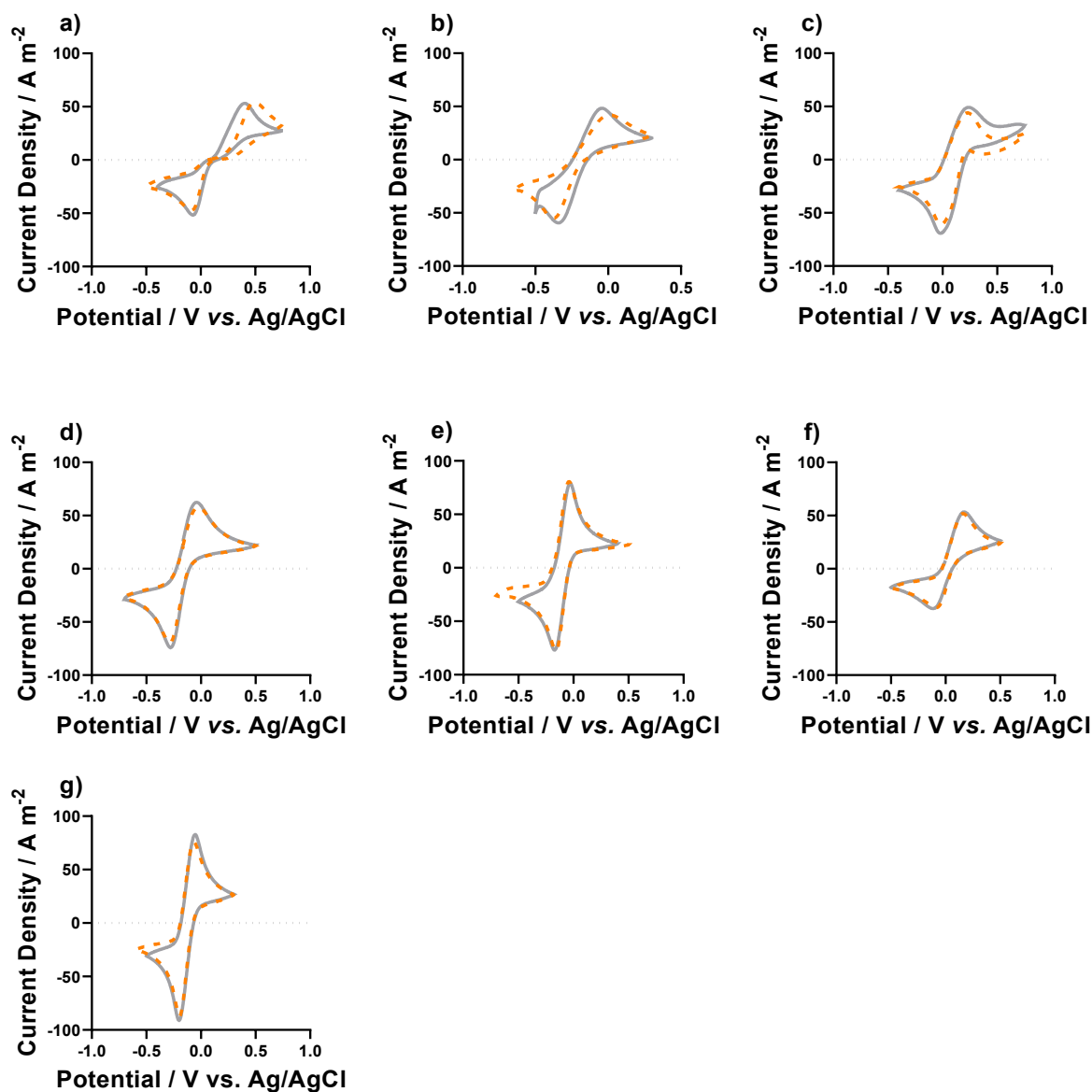


Figure S2 – Cyclic voltammograms (CVs) of all Fe(ligand) complexes at both Au (orange dashed) and Pt (silver solid) electrodes (both 1.6 mm in diameter, at a scan rate of 50 mV s⁻¹) for (a) Fe(Ac), (b) Fe(Mal), (c) Fe(IDA), (d) Fe(NTA), (e) Fe(EDTA), (f) Fe(EGTA), (g) Fe(DEPTA). At a scan rate of 50 mV s⁻¹, against a Ag|AgCl reference electrode. The concentration of Fe in these solutions were 100 mM total (*i.e.*, 50 mM of Fe(ii) and 50 mM of Fe(iii)), with the ratio of Fe : carboxylate acid ligand : carboxylate ligand described in Table 1 in the main text

Electrochemical Analysis Figures

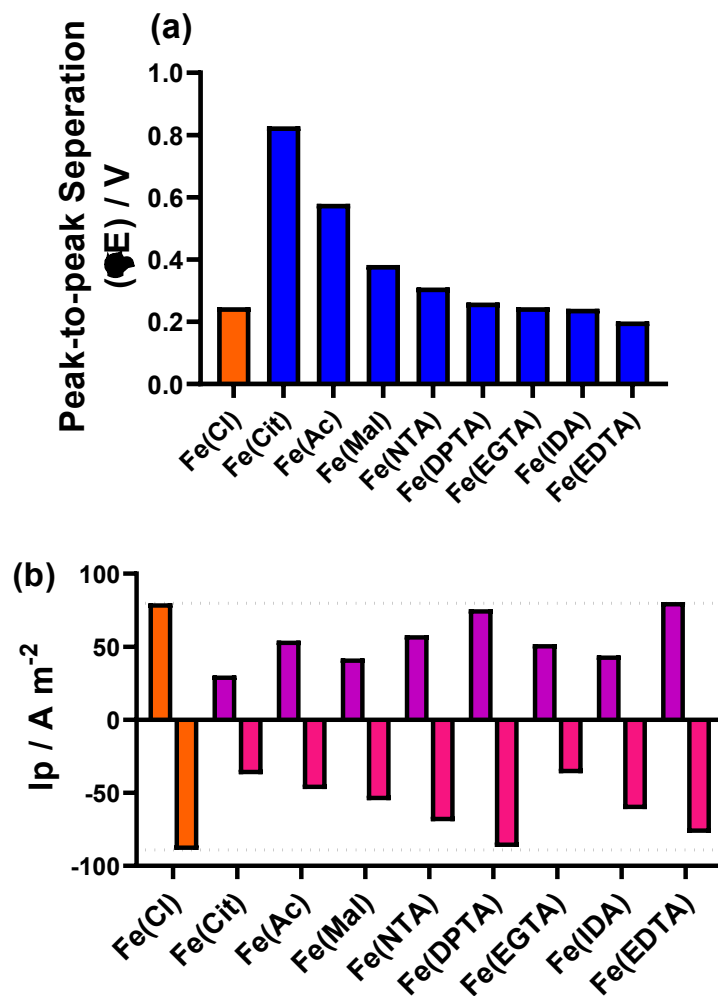


Figure S3 – Bar charts showing the cyclic voltammetric a) peak-to-peak separation (ΔE) and b) peak current density (j_p) of all redox couples investigated here, measured from the CVs shown in Figure 3.

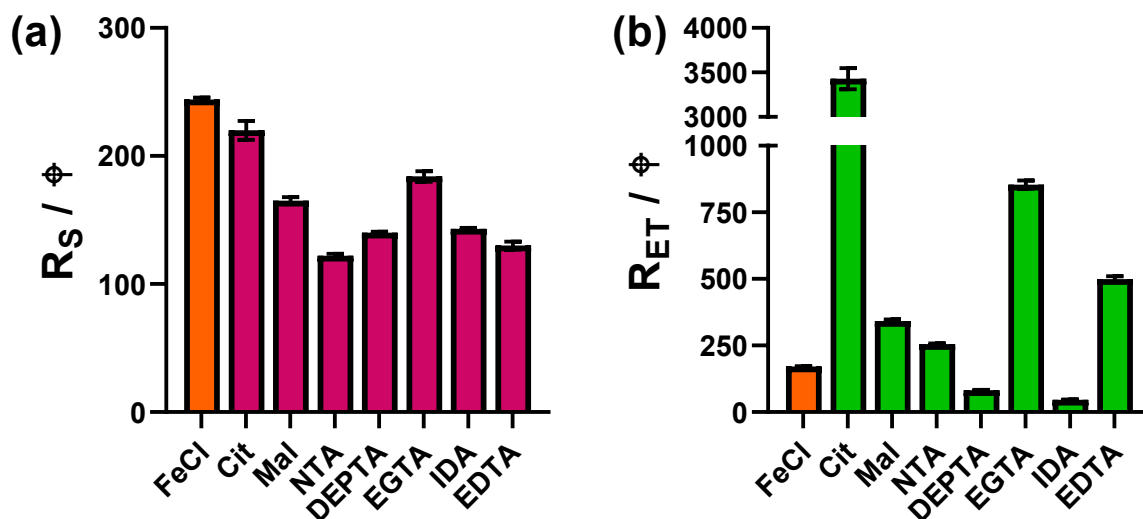


Figure S4 – Bar charts showing the inherent resistances measured by electrochemical impedance spectroscopy, showing a) the solution resistance (R_s) and b) electron transfer resistance (R_{ET}). The equivalent circuit used, and the Nyquist plots are all shown in Figure S5. Measured at Pt electrodes *ex-situ* of the thermocell at isothermal temperature.

Nyquist plots of the Electrochemical Impedance Spectroscopy on Pt.

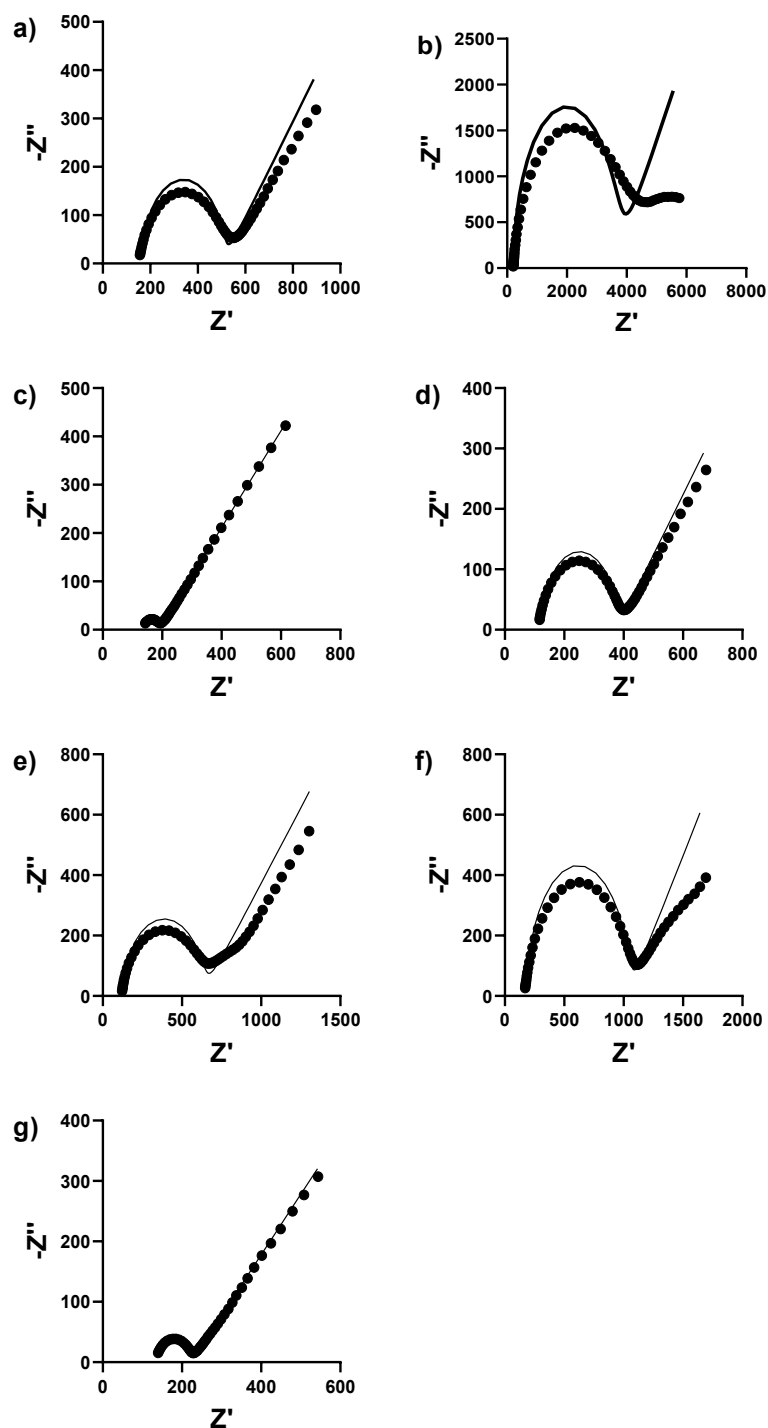
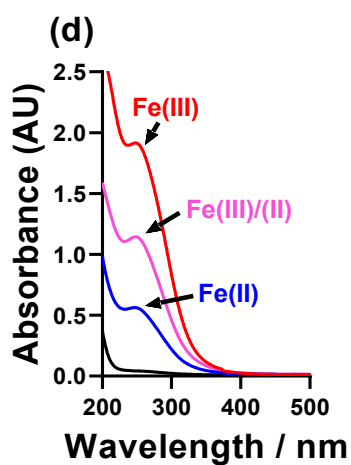
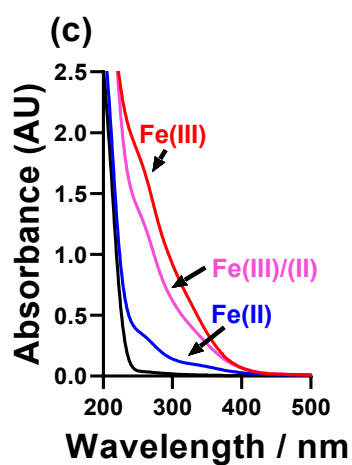
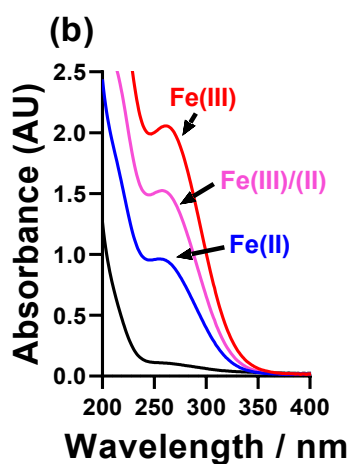
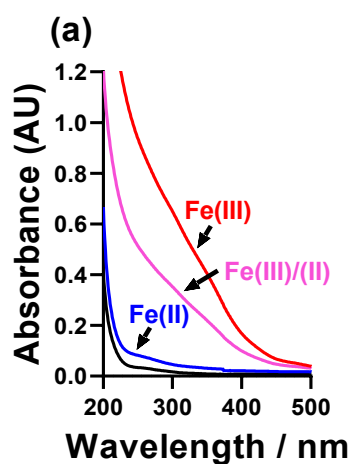


Figure S5 – Nyquist and fitting plots for all investigated Fe(ligand) systems (with the exception of Fe(Ac) which could not be rationally fit. These have been fit using a typical (R(RC)) model used previously.¹ For (a) Fe(Mal), (b) Fe(Cit), (c) Fe(IDA), (d) Fe(NTA), (e) Fe(EDTA), (f) Fe(EGTA) and (g) Fe(DEPTA). These were conducted using a Pt-working electrode of 1.6 mm *ex-situ* of the thermocell. Impedance spectra was recorded from 20,000 to

0.1 Hz with an amplitude of 10 mV. The solution composition was 100 mM of Fe in total (i.e. 50 mM of Fe(ii) and 50 mM of Fe(iii)) in the ratio of Fe : carboxylic acid ligand : carboxylate ligand as per Table 1 in the main text. The lowest Z' values represent the highest measured frequency and the lowest Z' value represents the highest measured frequency.

UV-Vis



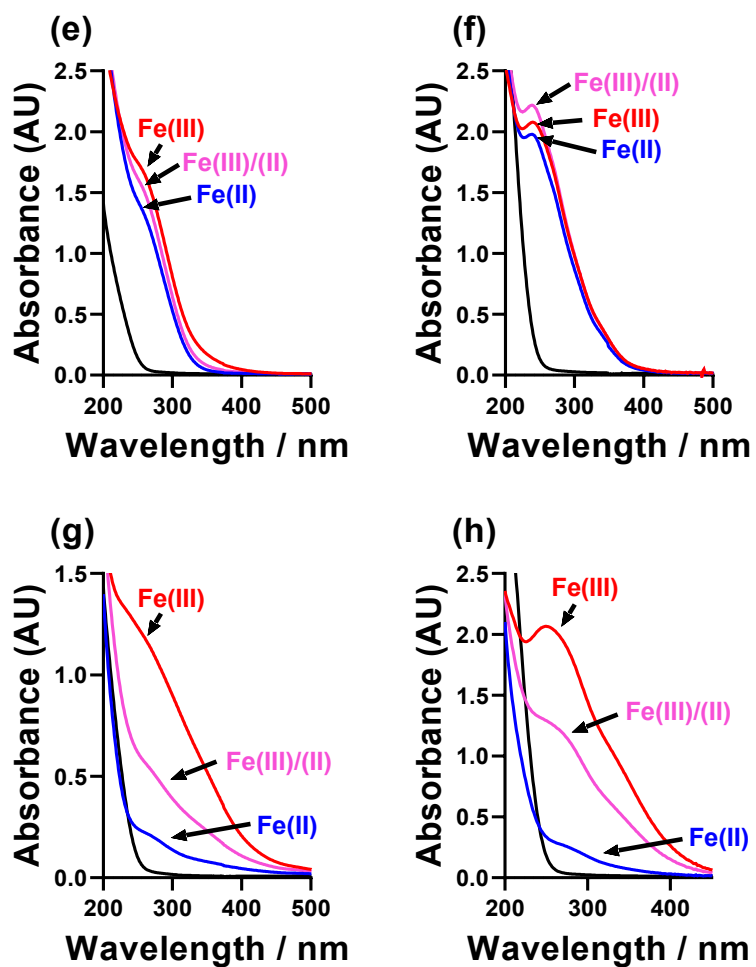


Figure S6 – UV-Vis spectra of Fe(iii), Fe(ii) alone or Fe(iii)/(ii) combined solutions of (a) Fe(Ac), (b) Fe(Mal), (c) Fe(Cit), (d) Fe(IDA), (e) Fe(NTA), (f) Fe(EDTA), (g) Fe(EGTA) and (h) Fe(DEPTA). Where the total Fe concentration is always 2.5 mM and the ratio of Fe : free acid : sodium carboxylate is shown in Table 1 in the main text.

Weaver plot with un-pH optimised Fe(EDTA), Fe(NTA) and Fe(DEPTA)

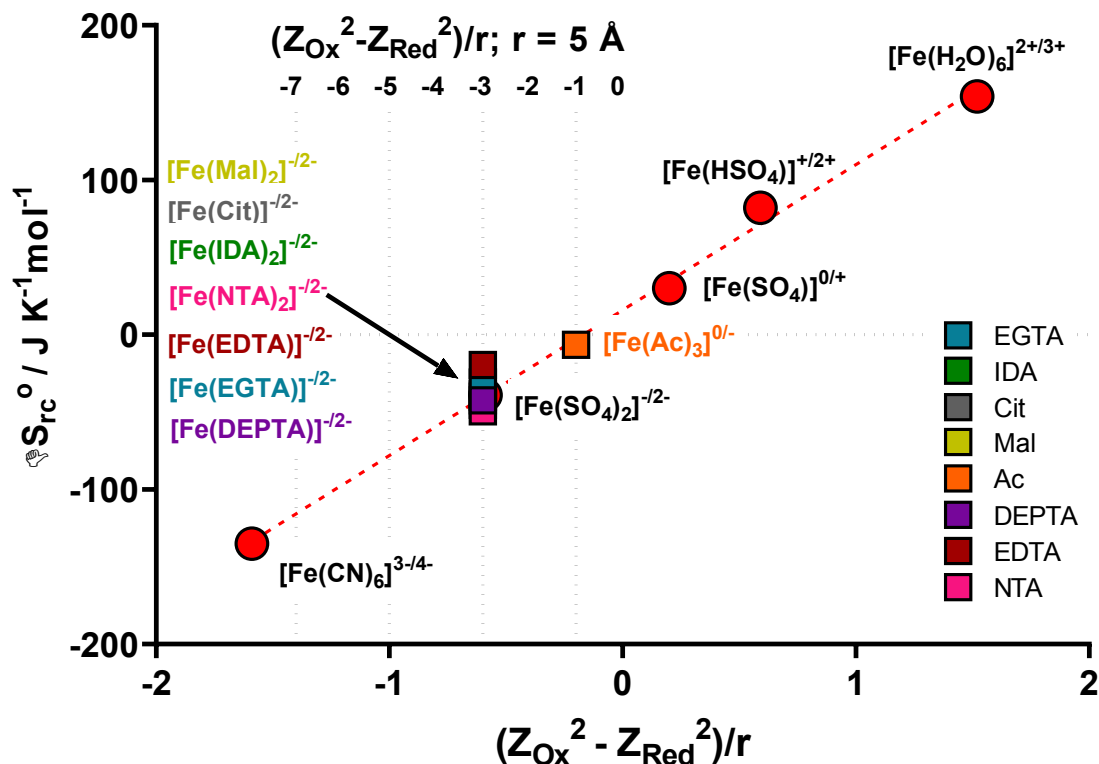


Figure S7 – Figure showing a plot of ΔS_{rc} vs. $(Z_{Ox}^2 - Z_{Red}^2)/r$ for all reported aqueous Fe(II)/Fe(III) redox systems (red circles) and all investigated Fe(ligand) solutions investigated here (coloured squares). The dotted lines indicate the $(Z_{Ox}^2 - Z_{Red}^2)$ values to 0/-1, -1/-2, -2/-3 and -3/-4 redox couples (using $r = 5 \text{ \AA}$). From these the likely ionic charge changes in the redox couples have been put next to the complex, e.g. $[\text{Fe}(\text{NTA})_2]^{3-/4-}$. The values for Fe(EDTA), Fe(DEPTA) and Fe(NTA) were the pH unoptimised values taken from Table 1 in the main text.

Determination of the structure of the Fe(ligand) complexes by Avogadro energy minimisation

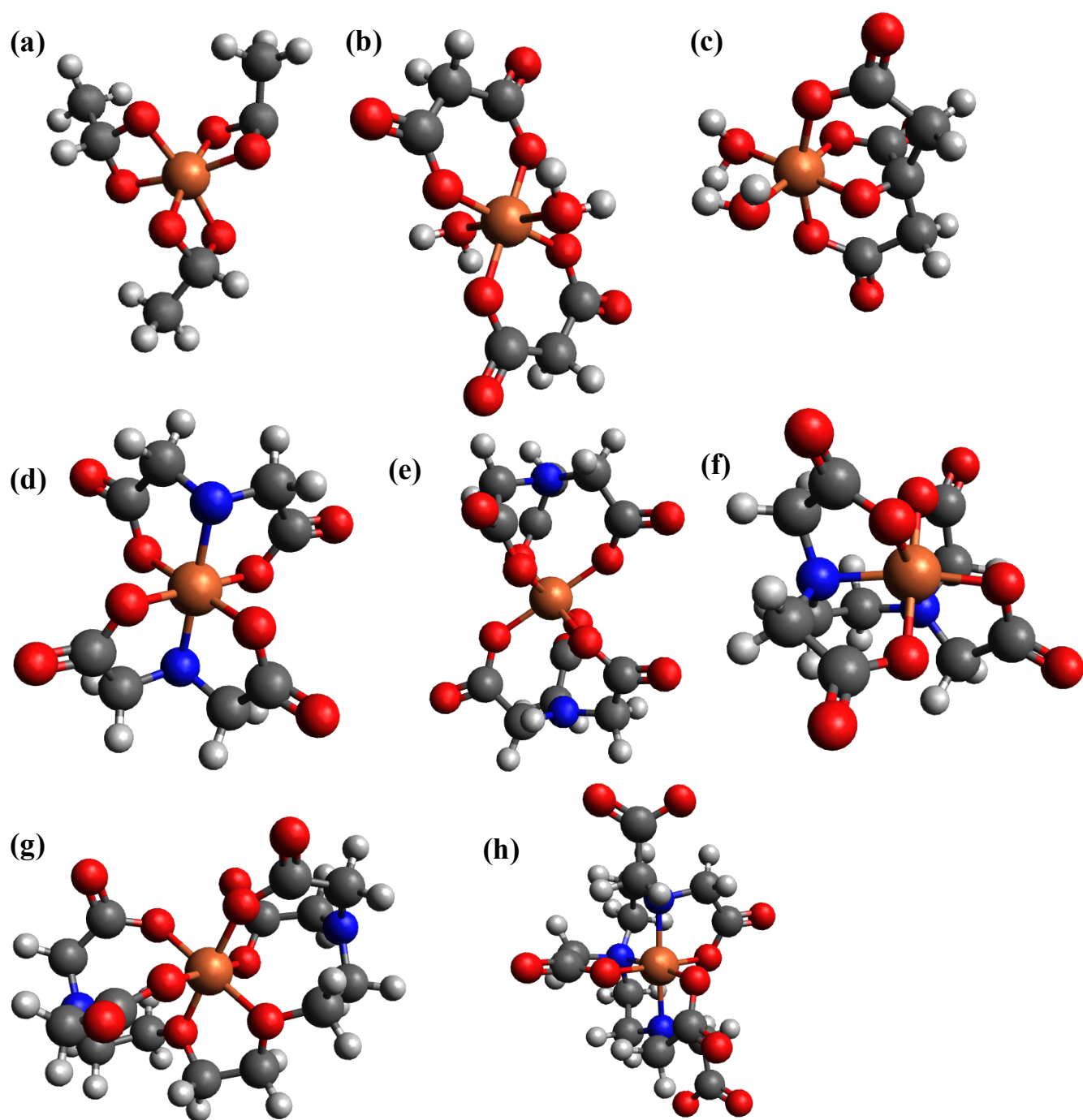


Figure S8 – Energy minimised conformational structures a) $[\text{Fe}(\text{Ac})_3]^{3-/4-}$ b) $[\text{Fe}(\text{Mal})_2(\text{OH}_2)_2]^{-/2-}$ c) $[\text{Fe}(\text{Cit})(\text{OH}_2)_2]^{-/2-}$ d) $[\text{Fe}(\text{IDA})_2]^{3-/4-}$ e) $[\text{Fe}(\text{NTA})_2]^{3-/4-}$ f) $[\text{Fe}(\text{EDTA})]^{-/2-}$ g) $[\text{Fe}(\text{EGTA})]^{-/2-}$ h) $[\text{Fe}(\text{DETPA})]^{2-/3-}$

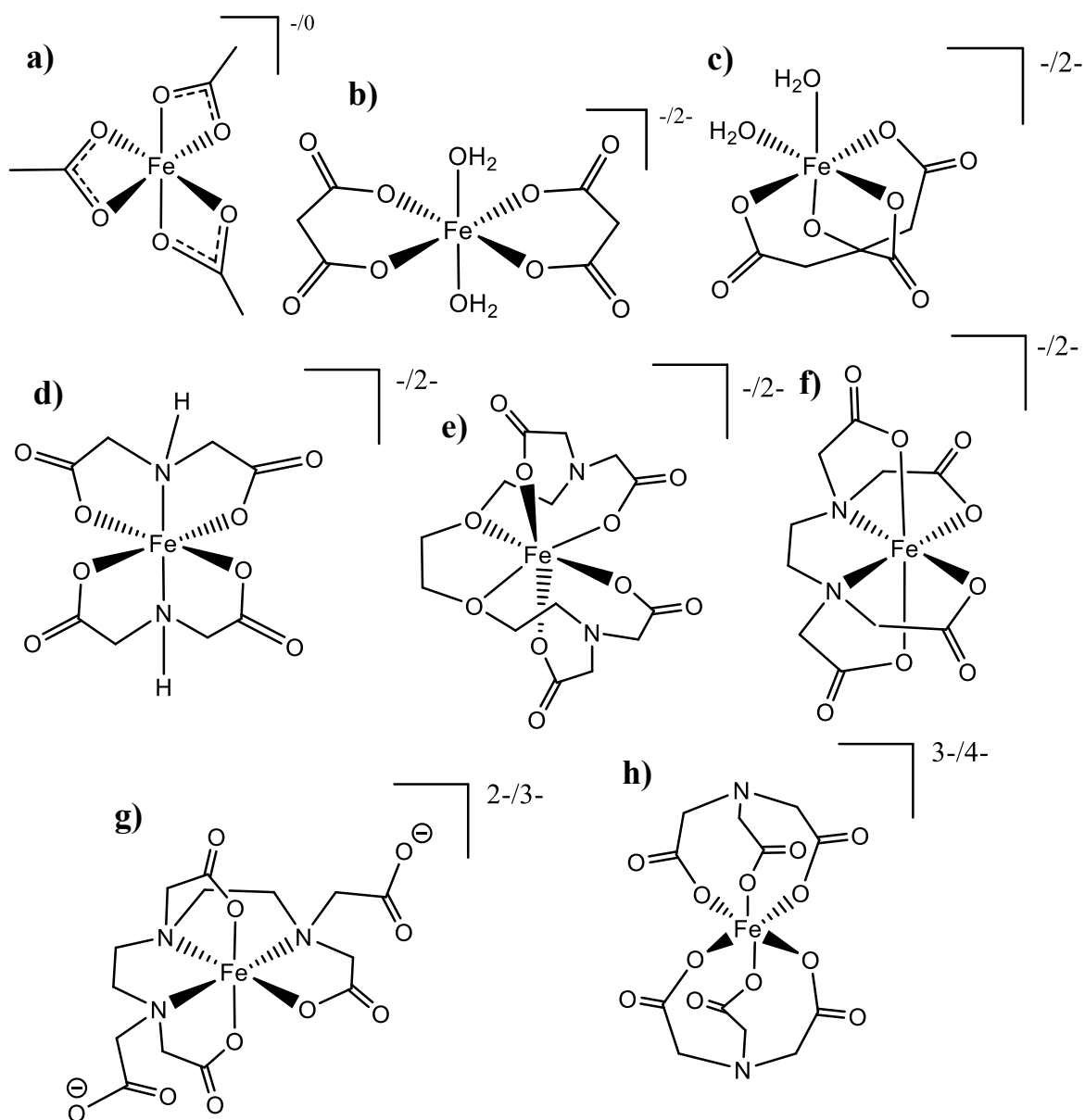


Figure S9 – Structures of the various iron-ligand complexes, where the ligand corresponds to those shown in Figure S1. Structures shown are those of the Avogadro energy minimised structures shown in Figure S8.

Table of Costing for cost : power analysis

Table S4 – A more detailed breakdown of numbers used for analysis in Table 3 in the manuscript. The Cost:Power ratio is for an arbitrary one second generation of power, under steady-state discharge conditions.

Fe(Ligand)	Power / mW	Cost of Materials per thermocell / £	Cost of Materials per thermocell (NaOH neutralised) / £	Cost : Power Ratio / £ mW ⁻¹	Cost : Power Ratio (NaOH Neutralised) / £ mW ⁻¹
Fe(Ac)	7.76 x10 ⁻⁷	0.0019	0.0013	2415.90	1732.00
Fe(Mal)	9.00 x10 ⁻⁵	0.1133	0.0047	1257.70	52.70
Fe(Cit)	1.93 x10 ⁻⁵	0.0043	0.0038	224.50	199.40
Fe(IDA)	5.17 x10 ⁻⁵	0.0224	0.0017	432.00	32.80
Fe(NTA)	1.52 x10 ⁻⁴	0.0053	0.0051	35.20	33.80
Fe(EDTA)	1.03 x10 ⁻⁵	-	0.0048	-	467.70
Fe(EGTA)	2.37 x10 ⁻⁵	-	0.0461	-	1950.50
Fe(DEPTA)	1.15 x10 ⁻⁴	0.0047	0.0059	41.00	51.50
Fe(DEPTA)	2.05 x10 ⁻⁴	0.0058	0.0070	28.00	33.80

Table S5 – Table of data for the cost analysis which is shown in Table 3 in the main text, showing the chemical, pack size and cost used. These were all taken from sigma aldrich website accessed 17th of June 2021.

Chemical	Grade (purity)	Cost / £	Pack size / g (or mL is specified)
Iron(iii) chloride	Reagent Grade (97%)	46.50	1000
Iron(ii) chloride tetrahydrate	ReagentPlus (98%)	114.00	1000
Iron(iii) sulphate	ACS Reagent (>99.0%)	55.40	1000
Iron(ii) sulphate	(97%)	107.00	500
Acetic acid	Glacial, ACS (>99.7%)	49.80	2500 (mL)
Sodium acetate trihydrate	ReagentPlus (>99.0%)	47.70	1000
Malonic acid	ReagentPlus (99%)	82.50	500
Disodium malonate hydrate	BioXtra	47.20	25
Citric acid hydrate	ACS (>99.0%)	40.60	1000
Trisodium citrate trihydrate	ACS (>99.0%)	44.70	1000
IDA(H ₂)	(98%)	36.70	500
IDA(Na ₂)	(>95.0%)	38.70	50
NTA(H ₃)	ACS (>99.0%)	41.50	500
NTA(Na ₃)	Sigma grade (>98%)	45.40	1000
EDTA(H ₄)	ACS Reagent (99.4-100.6%)	163.00	1000
EGTA(H ₄)	(>97.0%)	838.00	500
DEPTA(H ₅)	(>98%)	151.00	1000
DEPTA(Na ₅)	40% in water	35.50	500 (mL)
Sodium hydroxide	ACS (97%)	86.50	1000
Sodium sulphate	ACS (>99%)	89.60	1000
Potassium carbonate	ACS (>99%)	52.40	1000